

1972

FFM noise characterization of phase-locked impatt diode oscillators

Norman R. Dietrich
Lehigh University

Follow this and additional works at: <https://preserve.lehigh.edu/etd>

 Part of the [Electrical and Computer Engineering Commons](#)

Recommended Citation

Dietrich, Norman R., "FFM noise characterization of phase-locked impatt diode oscillators" (1972). *Theses and Dissertations*. 4007.
<https://preserve.lehigh.edu/etd/4007>

This Thesis is brought to you for free and open access by Lehigh Preserve. It has been accepted for inclusion in Theses and Dissertations by an authorized administrator of Lehigh Preserve. For more information, please contact preserve@lehigh.edu.

FM NOISE CHARACTERIZATION OF PHASE-LOCKED IMPATT DIODE OSCILLATORS

Norman R. Dietrich

ABSTRACT

A technique has been developed to carefully measure the power-noise characteristics of IMPATT oscillators. The objective being to determine their suitability as power amplifiers in the transmitters of frequency modulated radio-relay systems. The measured characteristics are used in conjunction with calculated performance contours for a typical repeater. The performance of the overall system, in terms of message circuit noise, when using the characterized diode, may be readily predicted. A direct method is provided for studying the dependence of the diode power and noise characteristics on operating conditions. The conditions leading to optimum system performance are identified. In general, this optimum is a compromise between maximum power and minimum noise. It is shown that a single IMPATT diode operating as a phase-locked oscillator can deliver sufficient power with low enough noise for short-haul radio-relay systems. The operating conditions which result in minimum noise or maximum power are also identified for applications where they are appropriate.

The technique provides the circuit designer with the information necessary to choose between diodes of different designs or materials and also yields insight and information valuable toward optimizing the overall system performance. The suitability of these devices for a specific radio-relay application depends upon the requirements of that system and the capabilities of the available diode designs.

FM NOISE CHARACTERIZATION OF PHASE-
LOCKED IMPATT DIODE OSCILLATORS

by

Norman R. Dietrich

A Thesis

Presented to the Graduate Committee

of Lehigh University

in candidacy for the Degree of

Master of Science

in

Electrical Engineering Department

Lehigh University

1972

This thesis is accepted and approved in partial fulfillment
of the requirements for the degree of Master of Science.

March 8. 72.

(date)

James C. Lehman

Professor in Charge

AK Furbush

Chairman of the Department

ACKNOWLEDGMENTS

The author expresses appreciation to Professor Walter E. Dahlke of Lehigh University for his guidance and to colleagues at Bell Laboratories for their advice. Dr. I. Tatsuguchi contributed to the development of the described techniques. Dr. C. B. Swan, in addition to his many technical contributions reviewed the manuscript and provided encouragement toward its completion. R. L. Sweet performed the system performance calculations and Dr. J. W. Gewartowski reviewed the manuscript.

TABLE OF CONTENTS

	<u>Page</u>
ABSTRACT	1
SECTION 1 INTRODUCTION	2
SECTION 2 THE PHASE-LOCKED OSCILLATOR	4
2.1 Summary of Section 2	4
2.2 Oscillator Circuit	4
2.3 Power and Noise of the Phase-Locked Oscillator	6
SECTION 3 NOISE MEASUREMENT TECHNIQUE	9
3.1 Summary of Section 3	9
3.2 Noise Measuring Circuit	9
3.3 Circuit Calibration	11
3.4 Factors Affecting Accuracy	15
3.5 Measured Results	19
SECTION 4 RADIO SYSTEM CHARACTERIZATION	21
4.1 Summary of Section 4	21
4.2 An Assumed Repeater Model	21
4.3 Calculation of Repeater Performance Contours	23
SECTION 5 THE PREDICTION OF SYSTEM PERFORMANCE	27
5.1 Summary of Section 5	27
5.2 Power-Noise Characteristics used to Predict System Performance	27
SECTION 6 CONCLUSIONS	29
REFERENCES	31
BIOGRAPHICAL SKETCH	33

LIST OF FIGURES

- Figure 1 State of the Art CW Power vs. Frequency.
- Figure 2 The Phase-Locked Oscillator.
- Figure 3 The Equivalent Circuit for the Single-Tuned Oscillator.
- Figure 4 A Family of Power-Noise Characteristics.
- Figure 5 Measuring Circuit Block Diagram.
- Figure 6 A Power Scale Relating Carrier and Noise Power Levels.
- Figure 7 Baseband Response of the Noise Measuring Circuit.
- Figure 8 Carrier Suppression Filter Response.
- Figure 9 Typical Measured Results.
- Figure 10 Results of the Accuracy Test.
- Figure 11 The Assumed System Model.
- Figure 12 Constant Performance Contours.
- Figure 13 The Prediction of System Performance.
- Figure 14 A Comparison of Several Diodes.

ABSTRACT

A technique has been developed to carefully measure the power-noise characteristics of IMPATT oscillators. The objective being to determine their suitability as power amplifiers in the transmitters of frequency modulated radio-relay systems. The measured characteristics are used in conjunction with calculated performance contours for a typical repeater. The performance of the overall system, in terms of message circuit noise, when using the characterized diode, may be readily predicted. A direct method is provided for studying the dependence of the diode power and noise characteristics on operating conditions. The conditions leading to optimum system performance are identified. In general, this optimum is a compromise between maximum power and minimum noise. It is shown that a single IMPATT diode operating as a phase-locked oscillator can deliver sufficient power with low enough noise for short-haul radio-relay systems. The operating conditions which result in minimum noise or maximum power are also identified for applications where they are appropriate.

The technique provides the circuit designer with the information necessary to choose between diodes of different designs or materials and also yields insight and information valuable toward optimizing the overall system performance. The suitability of these devices for a specific radio-relay application depends upon the requirements of that system and the capabilities of the available diode designs.

SECTION 1

INTRODUCTION

The IMPATT diode was proposed by W. T. Read¹ of Bell Laboratories in 1958. He predicted that a semiconductor junction having a localized high-field avalanche region followed by a moderately high-field drift region would exhibit a negative conductance characteristic at microwave frequencies and would be a powerful and efficient source of microwave energy. Demonstration of IMPATT operation was first reported in 1965 by Johnston, DeLoach and Cohen². Continuing effort in the development of IMPATT diodes has led to power levels and efficiencies of practical value.

Figure 1 shows state of the art power levels over a wide range of microwave and millimeter-wave frequencies obtained with silicon diodes by Bell Laboratories. (The intersection of dashed lines at the six GHz, one watt point identifies the area of interest in the present investigation.) The efficiency, when operated in the transit-time mode, is typically five to ten percent and can be as high as 15 percent for gallium-arsenide diodes.

Devices of this type have important potential applications in radio-relay systems: They can serve as CW signal generators supplying carrier or beat oscillator signals thus eliminating klystrons or frequency multiplier chains. They also perform as FM power amplifiers when operated as phase-locked oscillators.^{3,4} In this role, as the final amplifier in an FM radio relay transmitter,

they are a potential replacement for the traveling-wave tube; one of the long-time holdouts against an all solid-state radio-relay repeater. Prior to the development of the IMPATT diode, solid-state amplifiers of suitably low noise, high power and efficiency had not been available.

It is the purpose of this investigation to develop a procedure which measures the noise for phase-locked IMPATT oscillators and its dependence on operating conditions. By using power and noise measurements in conjunction with the characteristics of a model radio-relay system, a direct method for predicting system performance has been developed. The interdependence of output power and noise and their effect on the performance of the model radio-relay system can be explored. Information gained with the evaluation technique can also be used to compare the relative merits of various diode designs, to choose the optimum operating conditions for a given diode, or to aid in optimizing a diode design for a particular application. All measurements in this study relate to the application of IMPATT power amplifiers in the six GHz radio band. The techniques developed are generally applicable to other amplifying devices and to other radio systems.

SECTION 2

THE PHASE-LOCKED OSCILLATOR

2.1 Summary of Section 2

The phase-locked oscillator is discussed and the important operating parameters are identified in terms of an equivalent circuit. A power-noise characteristic using these parameters is presented.

2.2 Oscillator Circuit

Figure 2 shows a schematic diagram for a phase-locked oscillator used as an FM amplifier. The oscillator is capable of following the frequency deviations of the input, or locking signal, P_{LOCK} , over a frequency range $2\Delta f$. This locking range is determined from the expression⁵ shown in Figure 2, where Q_{ex} is the external Q. The output power from the oscillator, P_{OSC} , divided by P_{LOCK} is the amplifier gain. In principle, very large gains are possible although a practical limit of 25-30 dB may be imposed by output impedance match and isolation considerations.

The "free-running" oscillator frequency, f_o , is determined by the circuit impedance presented to the diode. Figure 2 shows typical variations in the output power and phase when the locking signal is deviated over the locking range. $\Delta\phi$ is the

difference in phase⁵ between input and output signals. To limit $\Delta\phi$ and control the resulting phase distortion, the locking range ($2\Delta f$) is usually made considerably wider than the maximum frequency deviation of the input signal. In an application involving a low-index FM radio relay system the frequency deviations are typically under 10 MHz. If 100 MHz is desired for Δf , six GHz for f_0 , and 20 dB for the gain, the external Q is limited to six from the expression in Figure 2. Values of 10 or less are often used. Operating in a low Q oscillator circuit, the IMPATT diode generates significant noise sidebands. These, of course, limit the usefulness of the amplifier since this noise represents an interference in the frequency sidebands of the FM system where the modulated intelligence is conveyed.

The diodes are operated in conventional single-tuned coaxial oscillator cavities. The theory of operation for oscillator circuits has been well treated in the literature;^{3,4,5} and will not be discussed in depth here. Figure 3 shows the equivalent oscillator circuit. The total equivalent load admittance presented to the diode, including the package parasitics, can be represented by a load conductance G_L , and a shunt susceptance, B_L . The value of the load conductance determines whether the device will behave as a stable amplifier, or as an oscillator. The negative conductance of the diode, G_w , is a function of the peak RF wafer voltage as determined from large signal admittance measurements.⁶ The

magnitude of the negative conductance typically decreases monotonically with increasing RF voltage. If the load conductance is greater than the maximum magnitude of the wafer conductance the device behaves as a stable amplifier. As the load conductance is decreased below this value the device oscillates with an RF wafer voltage determined by the point at which the load conductance and the magnitude of the wafer conductance are equal, ($G_L + G_W = 0$). With no input signal applied the oscillator will "free run" at the frequency at which the load susceptance and diode susceptance, B_W are of equal magnitude and opposite sign, ($B_L + B_W = 0$).

Both G_W and B_W are functions of bias current, RF wafer voltage, and frequency. Hence, provisions are included in the oscillator circuit for the adjustment of G_L and B_L . G_L and, consequently, the RF voltage are adjusted by changing the characteristic impedance Z_0' , of the quarter-wave transformer shown in Figure 3. B_L and, consequently, the free running frequency are controlled by changing the position of the transformer which varies the line length, l . The adjustments are slightly interdependent.

2.3 Power and Noise of the Phase-Locked Oscillator

The phase-locked oscillator can be represented by a power generator and a noise generator. The output power is the sum of the input locking signal and the power generated by the diode, and may be expressed in terms of the wafer voltage and conductance. Hence, the output power will be a function of the load conductance,

as well as of the bias current and frequency. The noise generated by the diode will also be a function of these parameters. It has been observed,⁷ for example, that the noise varies as the load conductance is varied to change the power output from the device.

Noise measurements have normally been reported for the small signal stable amplifier conditions, while power measurements are made under large signal conditions. The objective here is to investigate the interdependence of the power and noise as a function of circuit operating conditions.

Families of performance characteristics can be generated in terms of the power output and FM noise with transformed load resistance (R_L) and bias current (I) as parameters. An example characteristic obtained in this study is shown in Figure 4. With the oscillator phase-locked to a CW signal, the bias current is varied in increments and the output power and FM noise are measured for each of several values of R_L . At each new value of bias current, the free-running frequency of the oscillator was readjusted to keep it at the frequency of the CW locking signal. The change in bias current causes a small change in the wafer susceptance and the load susceptance must be adjusted to maintain a constant free-running frequency. The small change in the position of the transformer causes a small change in the conductance, G_L . Hence, for simplicity, the measurements were made for constant values of the transformed load resistance, R_L , instead of a constant conductance,

G_L . In Figure 4, the solid lines join points of constant current, and the dashed lines join points of constant transformed load resistance.

From Figure 4 it is evident that the operating conditions for minimum noise, or maximum power output are quite different. Minimum noise and maximum power cannot be achieved simultaneously. Optimum utilization of the diode requires the selection of operating conditions that produce the most favorable trade-off in power and noise for the given application. It requires a detailed knowledge of the system characteristics, and will differ for each system, or each new set of characteristics.

SECTION 3

NOISE MEASUREMENT TECHNIQUE

3.1 Summary of Section 3

The noise measuring circuit is described along with the calibration procedure and a discussion of noise units. Several sources of measurement error are identified, and the result of an accuracy test which incorporates corrections for these errors is shown.

3.2 Noise Measuring Circuit

The FM noise and output power were measured with the circuit shown in the block diagram of Figure 5. The CW locking signal was derived from a low noise klystron oscillator (Hewlett-Packard Model 618C). Measurements were generally made with a locking power level of +10 dBm corresponding to the FM power available in the intended amplifier application. The measurement of high carrier-to-noise ratios (low noise levels) is limited by the residual noise level of the circuit. To increase the measuring capability of the circuit, a carrier suppression technique is used. The output from the phase-locked oscillator is passed through a narrow band-stop filter. The filter consists of a TE_{011} mode cavity with a Q of approximately 5000. The carrier is selectively rejected by typically 20 dB, thus degrading the carrier-to-noise ratio. The carrier power level at the input to the mixer is readjusted to a predetermined maximum level (-23 dBm) which does not cause serious preamplifier gain compression. The increased level of the accompanying

noise can then be measured more readily in the presence of the unavoidable circuit residual noise. The amount of carrier suppression must be accounted for when interpreting the measured results.

The suppressed carrier, with its accompanying noise, is converted from RF to IF and amplified by a mixer-preamplifier, LEL Model CJC-7-8627. The coaxial wideband (4-8 GHz) mixer has a single-sideband noise figure of 8 dB. A gain of 20 dB, flat to within ± 0.15 dB over a 20 MHz band, is provided by the preamplifier. A narrow bandpass filter employing a TE_{011} mode cavity is used to prevent local oscillator noise from entering the mixer. The local oscillator is a Hewlett-Packard Model 618C signal generator. I.F. amplification, amplitude limiting, and frequency discrimination are provided by a Western Electric Model 4A FM receiver. The output from the FM receiver is a baseband AM noise spectrum, corresponding to the RF phase noise spectrum. The level of the baseband spectrum can be selectively analyzed as a function of frequency with the selective power meter (Hewlett-Packard Model 312A).

Noise levels within the relatively narrow sampling bandwidth of the selective power meter are measured at frequencies across the range of 0.5 to 10 MHz. This is the band in which information is carried in typical FM radio relay systems. It is assumed that the noise is uniformly distributed ("white") across the sampling band, and the noise level can be proportioned to any

chosen bandwidth. All noise measurements are referred to a one Hertz band in this study.

The noise power measured by the power meter is related to the FM noise generated by the IMPATT diode. It is, however, dependent upon the discriminator sensitivity as well as the frequency responses of the circuit components. Hence, to express the noise performance of the amplifier in terms of the familiar noise units, it is necessary to calibrate the circuit by relating the power meter reading to a known RF power level. The carrier-to-noise power ratio is determined and the known analytic expressions may be applied to relate to other units.

3.3 Circuit Calibration

The FM noise measuring circuit is calibrated by measuring the sideband power of a frequency modulated carrier having a known index of modulation, X . The reading on the selective power meter corresponds to a single-sideband carrier-to-noise ratio $(C/N)_{SSB-FM}$ as determined from the well known small signal FM relationships. The expression⁹ for a frequency modulated carrier is as follows:

$$M(t) = V_c \cos (\omega_c t + X \cos \omega_m t) \quad (1)$$

which may be written in the form:

$$M(t) = V_c \{ J_0(X) \cos \omega_c t + J_1(X) \cos [(\omega_c + \omega_m)t + \pi/2] + J_1(X) \cos [(\omega_c - \omega_m)t + \pi/2] + J_2(X) \cos [(\omega_c + 2\omega_m)t] + J_2(X) \cos [(\omega_c - 2\omega_m)t] + \dots \} \quad (2)$$

Where: V_c = carrier voltage amplitude

ω_c = carrier angular frequency

ω_m = modulation angular frequency

and, $J_{0,1,2,\dots}$ are Bessel functions with argument X , the index of modulation.

For very small (low index) modulation, e.g., $X = 0.1$:

$$J_0 = 0.998$$

$$J_1 = 0.050 (\approx X/2)$$

$$J_2 = 0.001$$

$$J_3 = 0.000$$

and (2) may be rewritten:

$$M(t) \approx V_c \left\{ \cos \omega_c t + \frac{X}{2} \cos [(\omega_c + \omega_m)t + \pi/2] + \frac{X}{2} \cos [(\omega_c - \omega_m)t + \pi/2] \right\} \quad (3)$$

The carrier power, C , is proportional to V_c^2 , and the sideband power, N , is proportional $(V_c \frac{X}{2})^2$.

Therefore:

$$C/N|_{SSB-FM} = \frac{V_c^2}{V_c^2 \frac{X^2}{4}} = \frac{4}{X^2} \quad (4)$$

Hence, if the index of modulation is known, the ratio of carrier to sideband power is also known.

For the low index modulated carrier to be used as a calibration signal the index of modulation is determined by observing the frequency spectrum on a spectrum analyzer. As the deviation is adjusted, the nulls of the carrier or sideband pairs are observed. These correspond to the zeros of the Bessel function coefficients in the expression for a frequency modulated carrier, (2). At these points, the values of the index of modulation, X , are accurately known from the tables of Bessel functions.

Thus calibrated, the circuit will measure the FM noise level at the output of a phase-locked oscillator relative to the output carrier power. The carrier-to-noise ratio may be expressed in dB and will apply specifically for FM noise present in a single-sideband of one Hertz width. The absolute level of the noise power is known since the output carrier level is readily measured. This may be referred to the input of the amplifier since the gain is also known. If the noise level accompanying the input locking signal is known, the device contribution may be separated and compared to thermal noise to determine the FM noise figure.

It must be recognized that the FM discriminators employed both in the measuring circuit and in the intended application are double-sideband detectors. Hence they will sum the upper and lower frequency sidebands. If the sideband signals are correlated in the FM sense the voltages will add. For uncorrelated sidebands the powers add. Since the calibrating signal is a frequency modulated

carrier the sidebands are correlated. The resulting calibration in terms of single-sideband carrier-to-noise ratio is correct for the case of correlated sidebands only. A signal with uncorrelated sidebands giving the same detected power level would have a $C/N|_{SSB}$ of 3 dB less. The noise sidebands at the output of a phase-locked oscillator are treated as being fully correlated,⁸ and the circuit calibration is correct as described. For any measurements involving thermal noise, the calibration must be corrected by 3 dB to account for the absence of correlation.

From the single-sideband carrier-to-noise ratio the equivalent double-sideband carrier-to-noise ratio may be determined. For the case of fully correlated sidebands:

$$C/N|_{DSB} = (1/4)C/N|_{SSB} \quad (5)$$

due to the voltage addition of the sidebands. Physically, $N|_{DSB}$ is the equivalent thermal noise in two sidebands which produces the same detected power level as produced by two sidebands of correlated noise. This noise level referred to the input of the device may be expressed as:

$$N_{DSB} = 2k(T_{eq} + T_o)B \quad (6)$$

where: k = Boltzmann's constant

B = 1 Hz bandwidth

T_{eq} = equivalent thermal noise temperature.

The noise figure, F , of an amplifier may be defined as the carrier-to-noise ratio at the input divided by that at the output, expressed in dB. It may be written:

$$F = 10 \log (1 + T_{eq}/T_o) \approx 10 \log T_{eq}/T_o \quad (7)$$

(for $T_{eq} \gg T_o$)

From expressions (5), (6), and (7), F may be written as:

$$F(\text{dB}) = 177 + P_{\text{LOCK}}(\text{dBm}) - C/N|_{\text{SSB}}(\text{dB}) \quad (8)$$

This relationship is illustrated on the power scale shown in Figure 6.

3.4 Factors Affecting Accuracy

a. Circuit Frequency Response

The calibration must be carried out at each frequency (f_m) of interest across the range of baseband frequencies unless the response of the circuit is flat, or well-known. In order to determine the response of the circuit a baseband signal of variable frequency and constant amplitude was modulated onto an I.F. carrier and up-converted to R.F. This signal was then measured by the noise measuring circuit for frequencies across the baseband, (.5 to 10 MHz). The results are shown in Figure 7. The roll-off of the circuit is about 1.3 dB at 10 MHz.

b. Effective Noise Bandwidth

A narrow bandpass filter in the selective power meter determines the bandwidth over which the noise power is measured.

As previously mentioned, the noise is proportioned to a one Hertz band. It is, therefore, necessary to know the effective noise bandwidth of this filter. This will differ from the half-power bandwidth since the shape of the filter characteristic is not ideal. The noise bandwidth of the power meter was determined by measuring the noise from a broadband random noise generator having a known spectral density.

The bandwidth, B, is given by:

$$B \text{ [Hz]} = \log^{-1} \frac{N_{\text{RDG}} - N(B)}{10} \quad (9)$$

where: N_{RDG} = the power reading, in dBm, on the selective power meter

$N(B)$ = the spectral density in dBm/Hz

For a specified 1000 Hz bandwidth on the instrument, the effective noise bandwidth was found to be 725 Hz.

c. Suppression Filter Response

The response of the carrier suppression filter must be known in order to determine its effect upon frequencies close to the carrier. Figure 8 shows the measured response of the filter. Corrections of 1.4 and 0.5 dB, as determined from this characteristic, are applied for noise measurements at one and two MHz respectively.

The phase characteristic of the filter must also be considered. If the two sidebands are shifted in phase by unequal amounts relative to the carrier the detected signal will be reduced. An asymmetrical phase characteristic due to improper tuning of the filter could cause an error at frequencies close to the carrier. At frequencies well removed from the cavity resonance the phase characteristic is less dependent upon frequency. The resonant frequency of the filter is tuned by observing the carrier power minimum with the power meter. It is essential to adjust the frequency of the suppression filter carefully, particularly for noise measurements below three MHz.

d. Circuit Residual Noise

The residual noise of the measuring circuit limits the sensitivity of the noise measurements. Obviously, the level of this noise must be negligible, or well known, with respect to the noise being measured. The sources of the circuit noise include the noise of the receiving system (primarily mixer noise), noise introduced from the local oscillator, and the noise of the locking signal source. The combined level of residual noise was measured with and without the use of carrier suppression. Figure 9 shows the results and illustrates the effectiveness of the carrier suppression technique. The carrier suppression is effective in reducing the relative level of the noise sources introduced beyond the point at which suppression is used. Noise added to the signal

prior to the suppression will not be altered. Hence, the noise of the locking signal source is fixed and it is the mixer and local oscillator contributions which are reduced. As a result the carrier suppression is more effective at frequencies removed from the carrier where the locking signal noise becomes negligible.

Figure 9 also shows the typical result for a silicon IMPATT diode oscillator measured using carrier suppression. Comparing this result to the residual noise measured without carrier suppression it is evident that the circuit noise would have added significantly to the measured noise. For frequencies close to the carrier the measured result approaches the residual noise in spite of the carrier suppression. If the residual noise is subtracted from the measured result the noise of the IMPATT oscillator is frequency independent across the range of interest. Hence, the measured noise at any frequency near the high end of the band of interest is representative of the noise performance of the oscillator, without the need for correction due to the residual noise level.

e. Verification of Measurement Accuracy

In order to verify the validity of the calibration procedure and corrections, a signal of known carrier-to-noise ratio was constructed, and measured. The known signal was constructed by combining a "clean" carrier with a known level of thermal noise power. The clean carrier was obtained by passing the CW signal

from a klystron through a narrow band-pass filter. The power level of the carrier is readily measured. The noise spectrum was derived from a traveling-wave tube amplifier with the input terminated by a 300°K load. The noise level was calibrated, at low level, against a noise lamp and increased to the desired level by adjusting a precision attenuator. The combined levels were set to a ratio of 130 dB. This test signal was then measured and the results are shown in Figure 10. The measurement was made using carrier suppression.

The measured results are corrected for the carrier suppression filter response. They are not corrected for the circuit residual noise nor the baseband roll-off. The effect of these is clearly evident from the curve. With these additional corrections applied the circuit measures within 1 dB of the expected result.

When performing this test, it must be recognized, however, that the noise being measured is now largely uncorrelated noise. Also, the very broad spectrum of noise extends to the image frequency of the mixer. The extra 3 dB of noise received at the image frequency compensates for the lack of correlation between upper and lower sidebands and the calibration does not require correction.

3.5 Measured Results

Using the circuit as described and calibrated and including the appropriate corrections, the noise of IMPATT diode

oscillators can be studied across the band of interest as a function of numerous operating parameters. In most instances, however, the noise at one frequency in the band of interest is representative. For the studies reported here in the form shown in Figure 4, the noise at 10 MHz from the carrier was used. At that frequency only the roll-off correction is required. The residual noise and carrier suppression filter phase and amplitude response corrections are insignificant.

SECTION 4

RADIO SYSTEM CHARACTERIZATION

4.1 Summary of Section 4

A model for a single hop of an FM radio-relay system and the equation for its thermal noise contribution are presented. Specific values for the operating parameters are taken from a typical system and the equation is used to compute performance contours for the model.

4.2 An Assumed Repeater Model

A single hop of a typical FM radio repeater system is shown in Figure 11. The assumed application is a transmitter amplifier replacement in an existing system design. Hence, some of the system parameters are predetermined:

Path Loss, $L_p = 2 \times$ antenna gain - air path loss (dB)

Amplifier Input Power, P_{IN} (dBm)

Microwave generator noise

Receiver noise

The variable parameters are those determined by the transmitter amplifier:

Power Transmitted, P_{OUT} (dBm)

Power Received, P_{REC} (dBm) = $P_{OUT} - L_p$

Transmitter amplifier noise

The basic formula^{10,11} for the thermal noise, W_N , of a repeater is:

$$W_N = 125.8 + P_S + 20 \log (f_m/\Delta F) + P_N - P_C \text{ dBrc0} \quad (10)$$

where:

P_S = test tone load capacity (dBm0)

f_m = baseband frequency

ΔF = single-frequency, peak frequency deviation corresponding to P_S

P_N = FM noise power at input (dBm/Hz)

P_C = input power (dBm)

Equation (10) holds for the thermal noise in a single message channel at baseband frequency, f_m , in a single radio hop using "C" message weighting. Its units are in dBrc0,¹¹ the standard unit in the Bell System for message circuit noise. The dBrc0 is a unit of message circuit noise power expressed in dB relative to a reference level of -90 dBm. The noise power is measured across the message circuit bandwidth with an instrument having a particular frequency response, i.e., "C" message weighting, and the level is referred to a reference transmission level in the circuit, 0 TLP.

Since FM radio systems use pre-emphasis to offset the inherent noise characteristics of FM modulation, an addition to Equation (10) must be made:

$$W_N = 125.8 + P_S + 20 \log (f_m/\Delta F) + P_N - P_C - \text{PRE} \quad (11)$$

PRE is the pre-emphasis advantage at the baseband frequency, f_m .

Equation (11) can be applied to the repeater as a whole or to its individual components. The noise from the individual components can then be added to yield the total repeater noise. It is assumed that the only significant contributions to noise are made at the low level receiving end and at the high level output end of the repeater. Thus, the only noise contributors considered are the transmitting amplifier and the receiver. The noise from the microwave generator is negligible for representative modern radio systems.

Let:

N_R = weighted noise of the receiver

N_{AMP} = weighted noise of the transmitting amplifier

N_{TOT} = weighted noise of the total repeater

Then:

$$N_{TOT} = N_R \text{ "+" } N_{AMP} \quad (12)$$

where "+" denotes power addition.

4.3 Calculation of Repeater Performance Contours

Typical values¹² for the parameters of an existing radio repeater system are:

$P_S = 26.0$ dBm0 for 1200 message circuit channel loading

$f_m = 564$ kHz to 5.772 MHz for 1200 message circuit channel loading, 5 MHz will be used here.

$\Delta F = 4$ MHz

$$L_p = 2 \times 40 - 143 = -63 \text{ dB}$$

$$\text{Receiver noise} = -166.2 \text{ dBm/Hz}$$

$$\text{PRE} = 2.2 \text{ dB at 5 MHz}$$

Substituting values for P_S , f_m , PRE and Δf into Equation (11), and simplifying:

$$W_N = 151.68 - P_C + P_N \quad (13)$$

Applying Equation (13) to the output amplifier:

$$\begin{aligned} N_{AMP} &= 151.68 - (P_C - P_N) \\ &= C_1 - (C/N)_{AMP} \end{aligned} \quad (14)$$

where:

$(C/N)_{AMP}$ is the carrier to SSB FM noise ratio of the output amplifier expressed in dB taken over a one Hz bandwidth.

For the receiver:

$$\begin{aligned} N_R &= 151.68 - P_{REC} + P_N = 151.68 + P_N + L_p - P_{OUT} \\ &= C_2 - P_{OUT} \end{aligned} \quad (15)$$

Only two variables are left unspecified, $(C/N)_{AMP}$ and P_{OUT} , and these are the design variables we wish to investigate. Solving for N_{TOT} using Equations (12), (14), and (15)

$$N_{TOT} = 10 \log \left[10^{(C_1 - (C/N)_{AMP})/10} + 10^{(C_2 - P_{OUT})/10} \right] \quad (16)$$

This equation gives the total repeater noise contribution in a given message circuit in terms of the carrier-to-noise ratio and power output of the transmitter amplifier, other parameters having been fixed by the system design. Figure 12 is a plot of this equation showing the trade-off between noise and power output for constant values of N_{TOT} ranging from 18 to 25 dBm/0. Each curve approaches an asymptote along both the ordinate and abscissa scales. Interestingly, the asymptote parallel to the abscissa gives the performance of the system when limited by the receiver noise. Improving the C/N (decreasing the noise) of the transmitter amplifier will not improve the repeater performance. An increase in transmitted power is necessary for improved system performance. The converse is true for the performance represented by the asymptote parallel to the ordinate. This represents a system where the transmitter noise is dominant.

It must be recognized here that the equation (14) giving the message circuit noise at baseband frequencies in terms of the RF single-sideband carrier-to-noise ratio already includes an assumption as to how the sidebands will be added by a double-sideband detector. The equation was derived for thermal noise which has no correlation between the upper and lower sidebands and would be added on a power basis, i.e., 3 dB increase in detected noise power due to the second sideband.

If the single-sideband carrier-to-noise ratio is measured as described in Section 3, it is also necessary to account for any correlation between sidebands before using equation (16) to predict the system performance. Since the device under investigation here is basically an oscillator it is assumed that the noise sidebands are fully correlated. Consequently, the sidebands would add on a voltage basis, i.e., an apparent 6 dB increase in detected noise power due to the second sideband. Hence, the message circuit noise contribution is 3 dB higher for a device having the same single-sideband carrier-to-noise ratio but having correlated sidebands. This is accounted for in the following section by offsetting the noise scales by 3 dB.

SECTION 5

THE PREDICTION OF SYSTEM PERFORMANCE

5.1 Summary of Section 5

It is shown that the power-noise characterization for the diode and the computed system performance contours may be used to predict repeater performance. Additional valuable information and insight is available for optimizing system performance.

5.2 Power-Noise Characteristics used to Predict System Performance

The results of the measurements and repeater characterization of the two previous sections can be combined to predict repeater performance. Also, valuable information can be gained toward the selection of operating conditions and optimization of diode designs. For example, Figure 13 is a plot of Figures 4 and 12 superimposed. The noise performance of the diode has been shifted (degraded) by 3 dB to account for the correlation of sideband noise as discussed in the previous section. From this plot it is clear that neither maximum output power, nor minimum noise are the desired conditions for best performance. Some combination of these interdependent quantities is better. For a given diode, the approximate values of the circuit parameters (R_L , I) which yield the best performance are clearly identified. Also, if the performance objective was specified as 22 dBrc0, for example, the ranges and possible combinations of these parameters which will allow the objective to be met are known.

This procedure can also be used to evaluate changes in a diode design or to compare diodes of various materials. Figure 14 shows such a comparison. The performance curves shown are the highest current curves representing the best measured performance for each diode. Even though the gallium-arsenide and the one silicon diode are capable of delivering equal output powers, the gallium-arsenide diode will provide 1 dB better repeater performance due to its lower noise. This would not necessarily be the case in an application where the repeater had a higher receiver noise figure. Better repeater performance with the gallium-arsenide diode could most readily be obtained with an increase in output power rather than a decrease in noise.

SECTION 6

CONCLUSIONS

The noise performance of IMPATT diode phase-locked oscillators and its dependence on operating conditions can be studied using the procedure described. The performance criterion is the noise present in a baseband message circuit. The suitability of these devices for applications as transmitter amplifiers must, of course, depend upon the nature and requirements of the intended system application. For short-haul radio relay routes a typical performance objective is 22 dBm/0 per hop. The diodes tested appear suitable as single-stage amplifiers. For long-haul operation, however, the noise per hop must be considerably lower. For such an application additional amplification would be required to meet the power output objectives (typically five to ten watts). The first stage of a multiple stage amplifier would operate under the conditions giving the best noise performance. The later stages would be optimized for best power output. The described procedure can be used to determine capabilities and to select the required operating conditions which allow the individual stages to meet these requirements.

The procedure developed here not only allows the prediction of repeater performance, but provides additional information useful in efforts to design or improve the system. It should be emphasized, however, that the procedure must be adapted

to each specific application in order to be useful. Each new system, or set of conditions for the same system will cause changes in the performance curves. In applications where significant AM-PM conversion takes place a similar study of the effects of AM noise should be undertaken.

REFERENCES

1. W. T. Read, "A Proposed High-Frequency Negative-Resistance Diode", Bell System Technical Journal, 37, 1958, pp. 401-446.
2. R. L. Johnston, B. C. DeLoach, Jr., and B. G. Cohen, "A Silicon Diode Microwave Oscillator", Bell System Technical Journal, 44, 1965, pp. 369-372.
3. M. E. Hines, "Negative-Resistance Diode Power Amplification", IEEE Transactions on Electron Devices, ED-17, January, 1970, pp. 1-8.
4. T. Isobe, M. Tokida, "A New Microwave Amplifier for Multichannel FM Signals Using a Synchronized Oscillator", IEEE Journal of Solid-State Circuits, SC-4, December, 1969, pp. 400-408.
5. K. Kurokawa, Theory of Microwave Circuits, New York, Academic Press, 1969, pp. 380-389.
6. D. R. Decker, C. N. Dunn, and R. L. Frank, "Large-Signal Silicon and Germanium Avalanche-Diode Characterization", IEEE Transactions on Microwave Theory and Techniques, MTT-18, Nov., 1970, p. 872-876.
7. A. M. Cowley, et al. "Noise and Power Saturation in Singly Tuned IMPATT Oscillators", IEEE Journal Solid-State Circuits, Vol. SC-5, pp. 338-345, December, 1970.

8. R. L. Kuvvas, "Noise in Single Frequency Oscillators and Amplifiers", to be published.
9. Bell Telephone Laboratories, Transmission System for Communications, Winston-Salem, North Carolina, Western Electric Company, Inc., Fourth Edition, 1970, pp. 452-453.
10. Ibid, pp. 480-482.
11. Ibid, pp. 31-34.
12. S. D. Hathaway, W. G. Hensel, D. R. Jordan, R. C. Prime, "TD-3 Microwave Radio Relay System", Bell System Technical Journal, Vol. 47, September, 1968, pp. 1149-1155.

BIOGRAPHICAL SKETCH

NORMAN RALPH DIETRICH - Born November 29, 1936 in rural Berks County, Pennsylvania. Parents names - Lillian Mae (Stump) and Ralph Jonas Dietrich. Married Ilabelle Rebecca (Wentzel), March 26, 1960. Three children: Lois Ann 9, Brian Scott 7, Gayle Dianne 3.

GRADUATE:

HAMBURG HIGH SCHOOL, Hamburg, Pa., May, 1954.

RCA INSTITUTES, New York, N. Y., Certificate in Electronic Technology, Honor Graduate, June, 1959.

LAFAYETTE COLLEGE, Easton, Pa. B.S.E.E., Cum Laude, June, 1966.

EXPERIENCE:

Employed by Bell Telephone Laboratories from June, 1959, to present. Assignments have been in the development of microwave components. These include traveling-wave MASER amplifiers for communications satellite ground station receivers, and circulators and microwave integrated circuits for radio-relay applications. Presently, Member of the Technical Staff in the Microwave Integrated Circuit and Amplifier Group, Allentown, Pa.

PUBLICATIONS:

1. "TH-3 Microwave Radio System: Microwave Integrated Circuits," Bell System Technical Journal, 50, No. 7, September, 1971.

2. "Power-Noise Characterization of Phase-Locked IMPATT Oscillators," IEEE Journal of Solid State Circuits SC-7, No. 1, February, 1972. (Coauthored with I. Tatsuguchi and C. B. Swan.)
3. "End Launch Stripline-Waveguide Transducer," U.S. Patent 3,483,489, December 9, 1969.

MEMBER:

The Institute of Electrical and Electronics Engineers.

Tau Beta Pi.

Eta Kappa Nu.

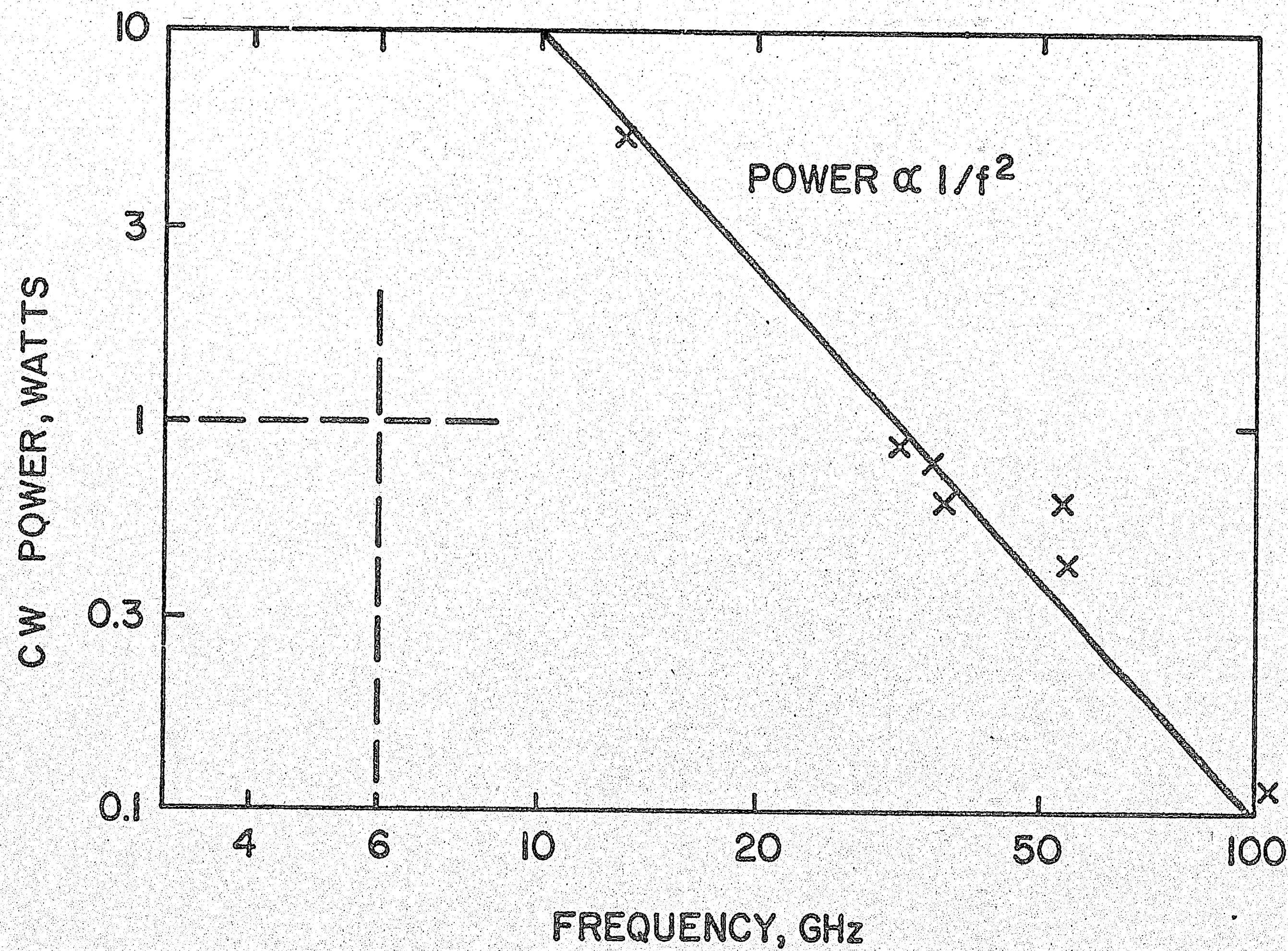
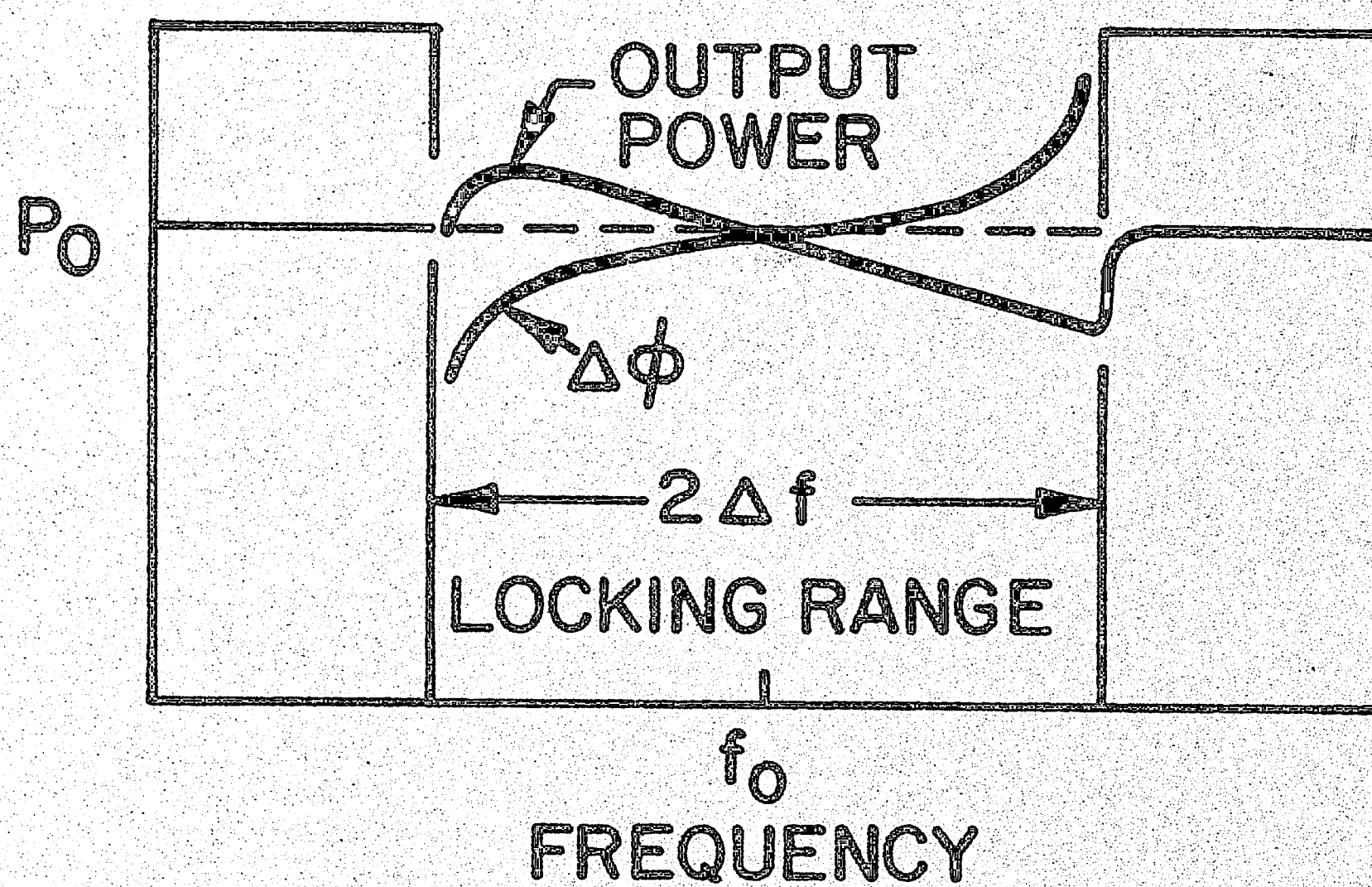
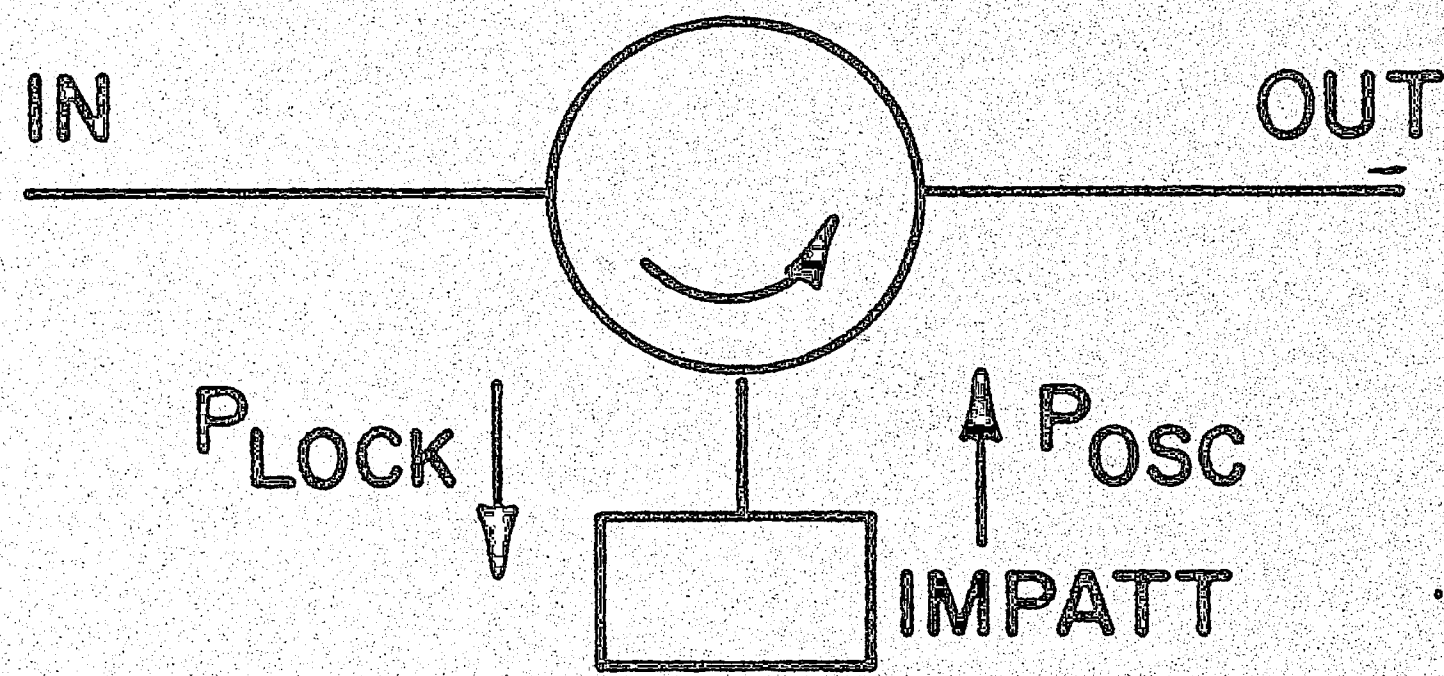


FIGURE 1 - State of the Art CW Power vs. Frequency. Points shown were obtained by Bell Laboratories with silicon IMPATT diodes. The limiting power levels follow a $1/f^2$ relationship. The six GHz, one watt point is the area of interest in this study.



$$\Delta f = \frac{f_0}{Q_{ex}} \sqrt{\frac{P_{LOCK}}{P_{OSC}}}$$

FIGURE 2 - The Phase-locked Oscillator. Typical output power and phase variations over the locking frequency band are shown. The expression relates the frequency, Q , power gain, and locking band for the phase-locked oscillator.

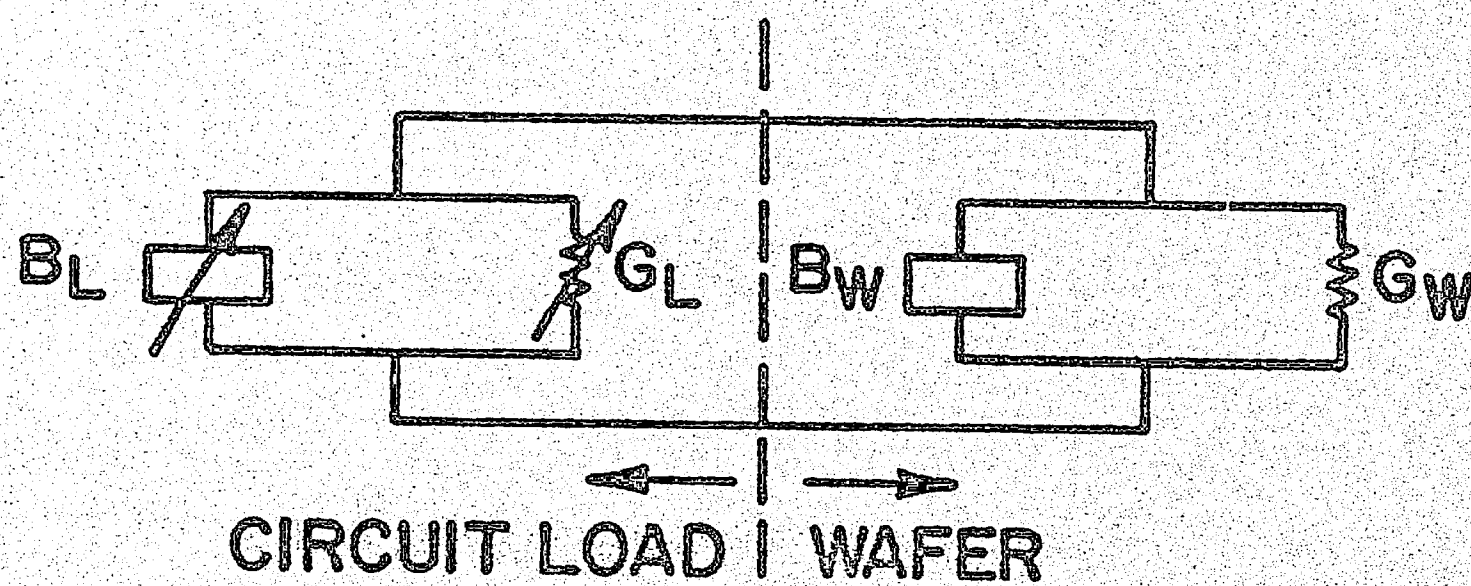
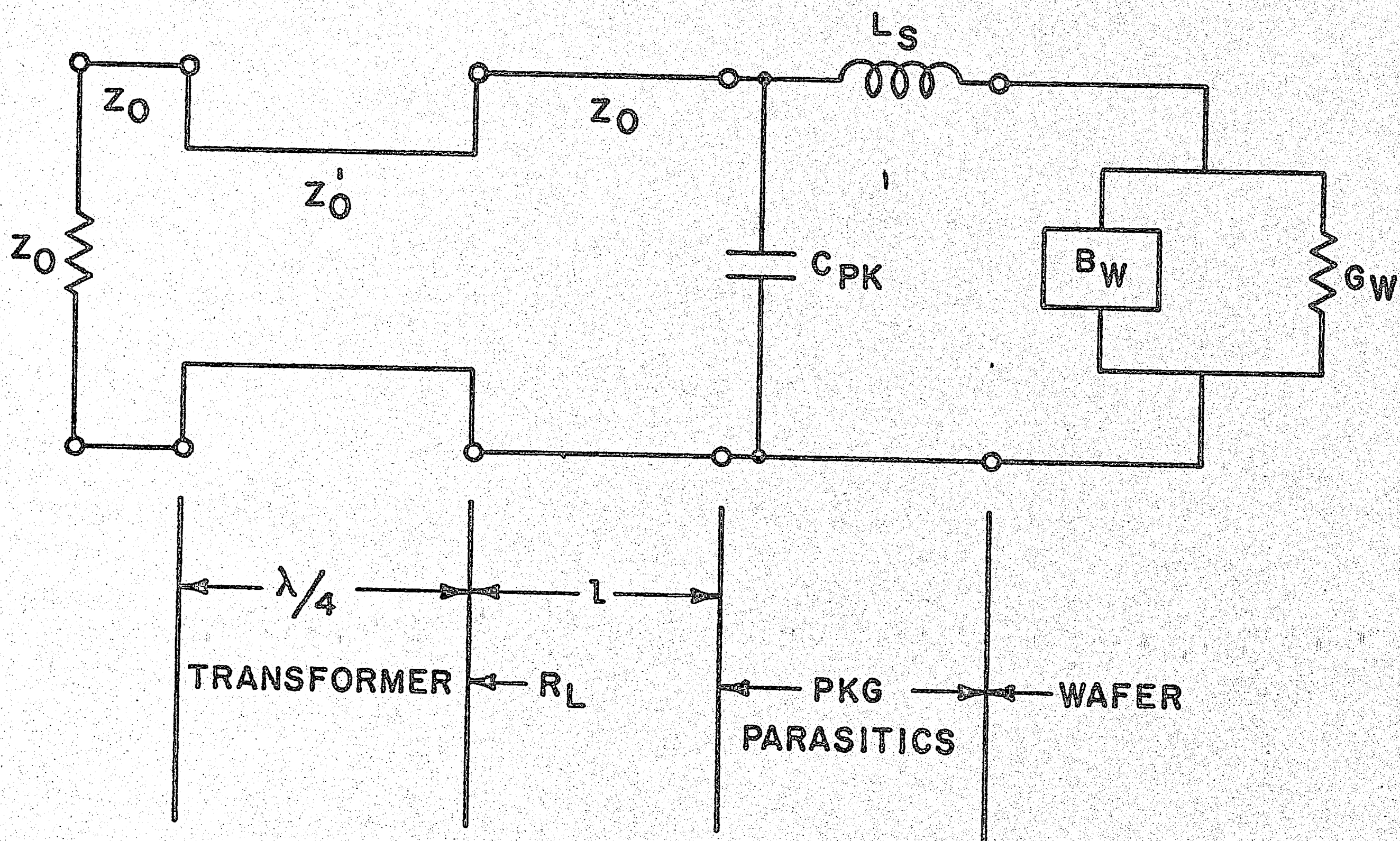


FIGURE 3 - The Equivalent Circuit for the Single-Tuned Oscillator. The wafer admittance, package parasitics, and circuit components are shown. R_L is the value of the transformed load impedance (a circulator) at the end of the movable quarter-wave transformer. The circuit and package parasitics may be combined into a variable circuit load admittance presented to the diode wafer.

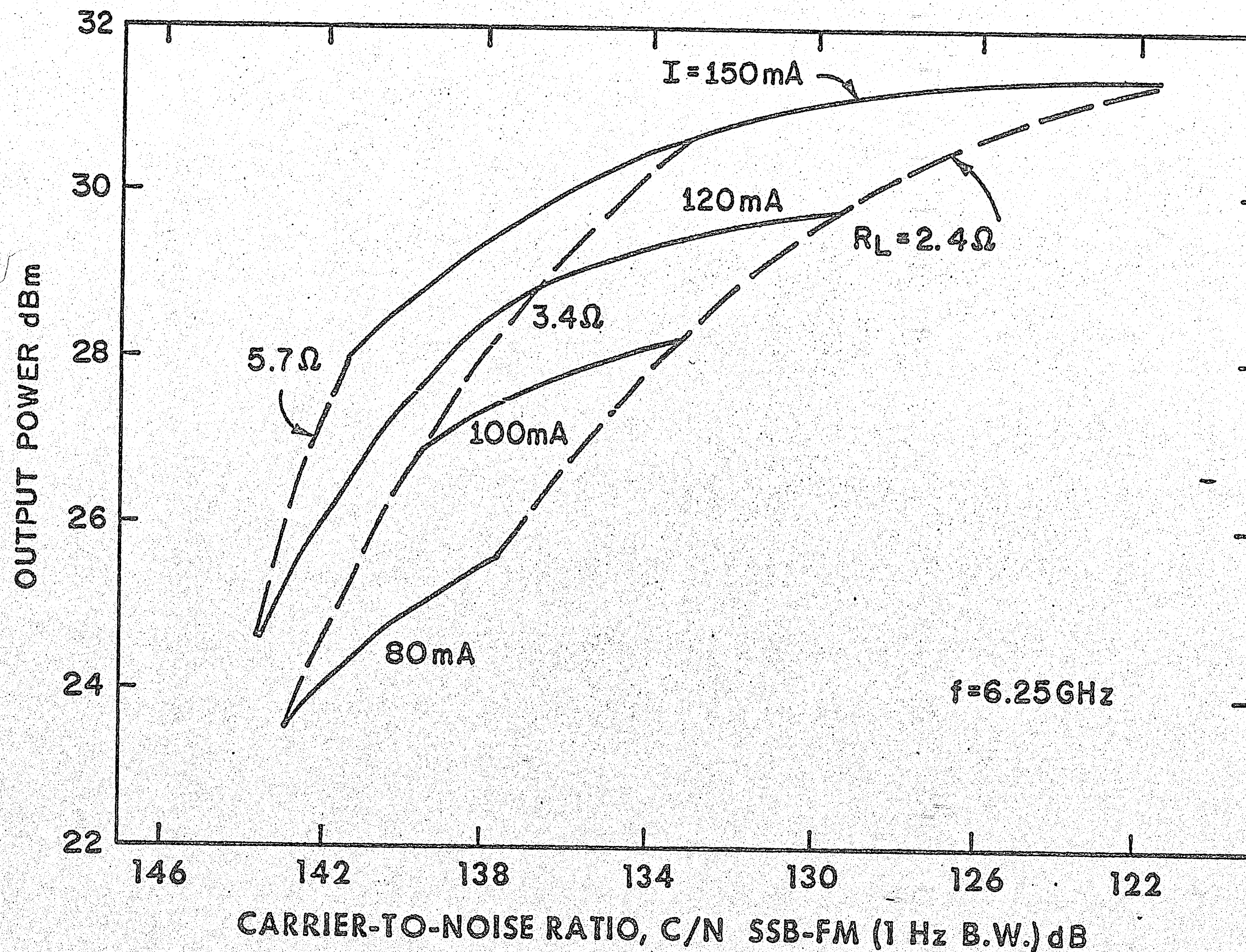


FIGURE 4 - A Family of Power-Noise Characteristics. The output power and noise were measured for a silicon IMPATT diode oscillator. The bias current was varied over the ranges shown for each of several values of transformed load impedance. The measurements were made with the oscillator phase-locked to a 6250 MHz signal. The free-running frequency was adjusted to 6250 MHz for all cases.

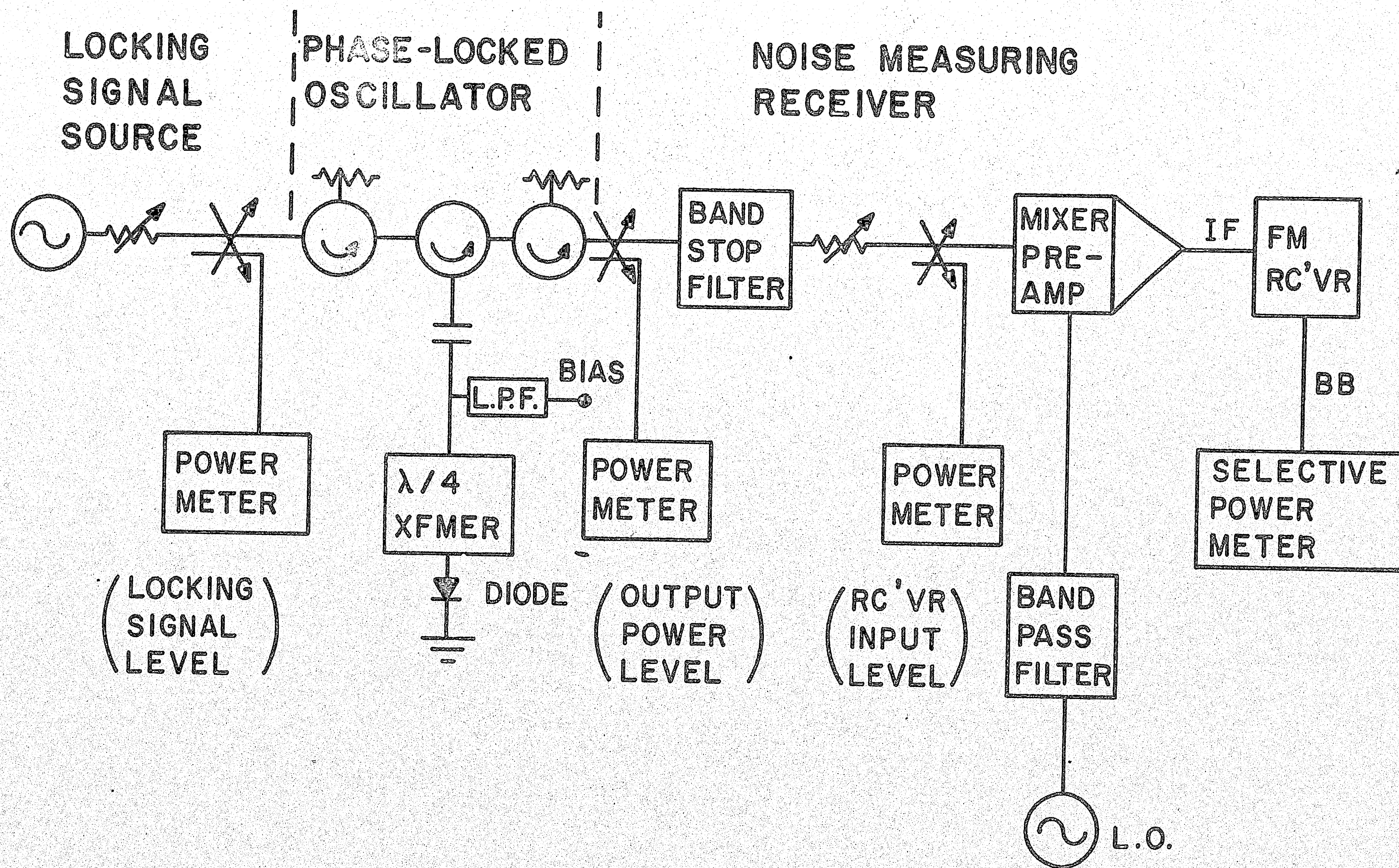
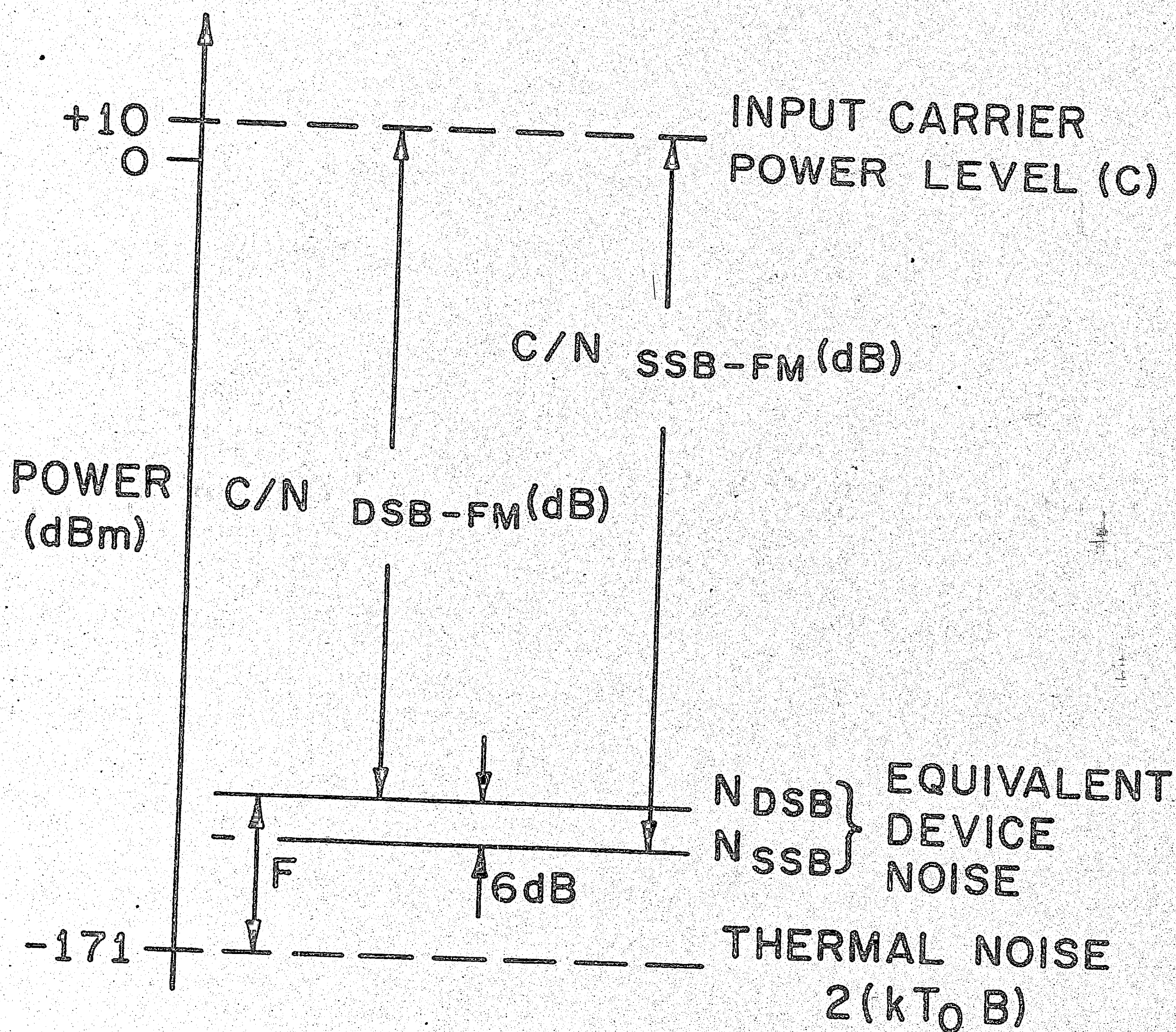


FIGURE 5 - Measuring Circuit Block Diagram. The power-noise characteristics were measured with the circuit shown.



$k = \text{BOLTZMANN'S CONSTANT}$

$B = 1 \text{ Hz BANDWIDTH}$

$T_0 = 290^\circ \text{K}$

FIGURE 6 - A Power Scale Relating Carrier and Noise Power Levels. The equivalent device noise is referred to the input of the device and taken over a one Hz band for the single-sideband case and two one Hz bands for the double-sideband case.

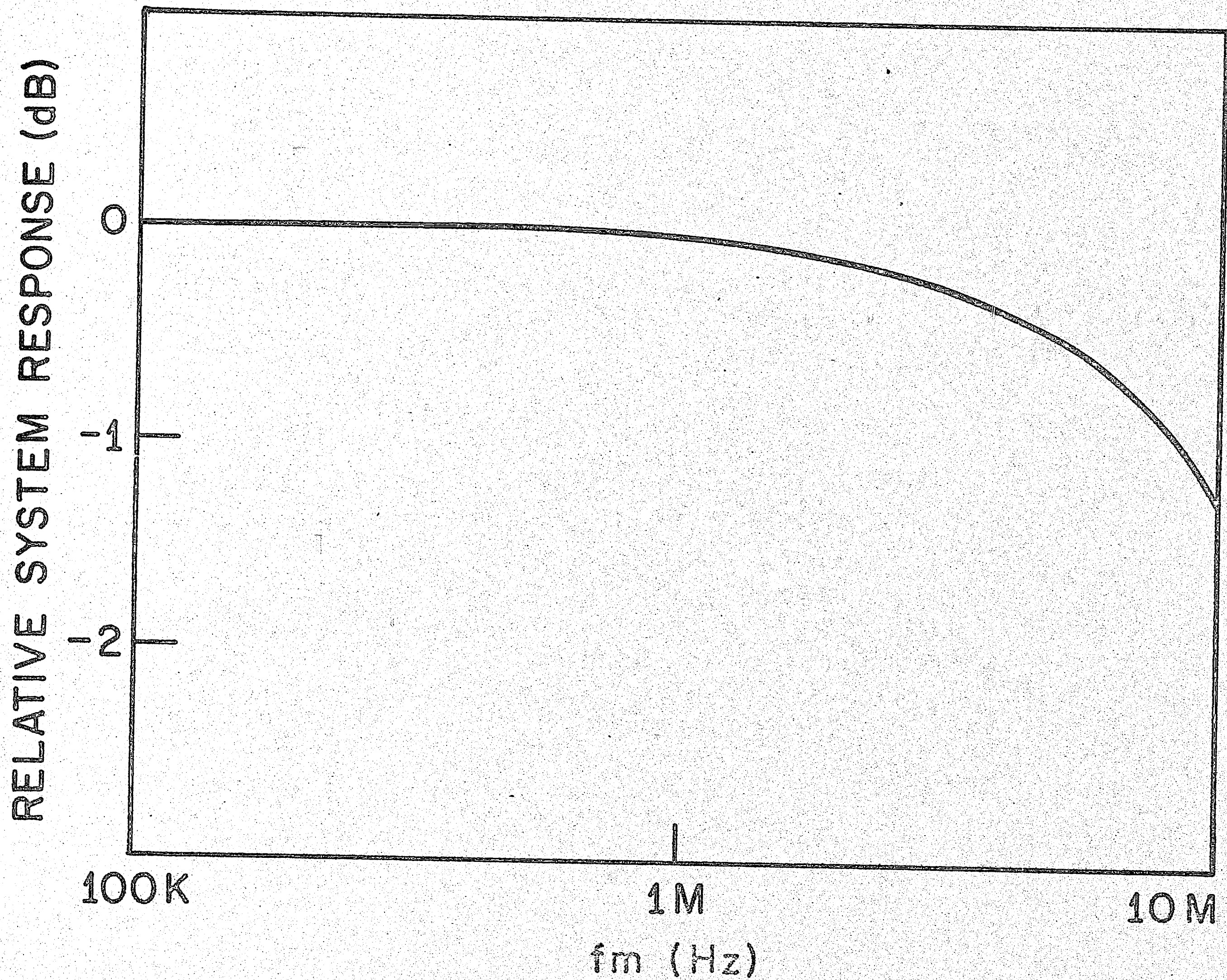


FIGURE 7 - Baseband Response of the Noise Measuring Circuit. The overall response of the circuit "rolls-off", and measured results must be corrected accordingly. The correction is 1.3 dB at 10 MHz.

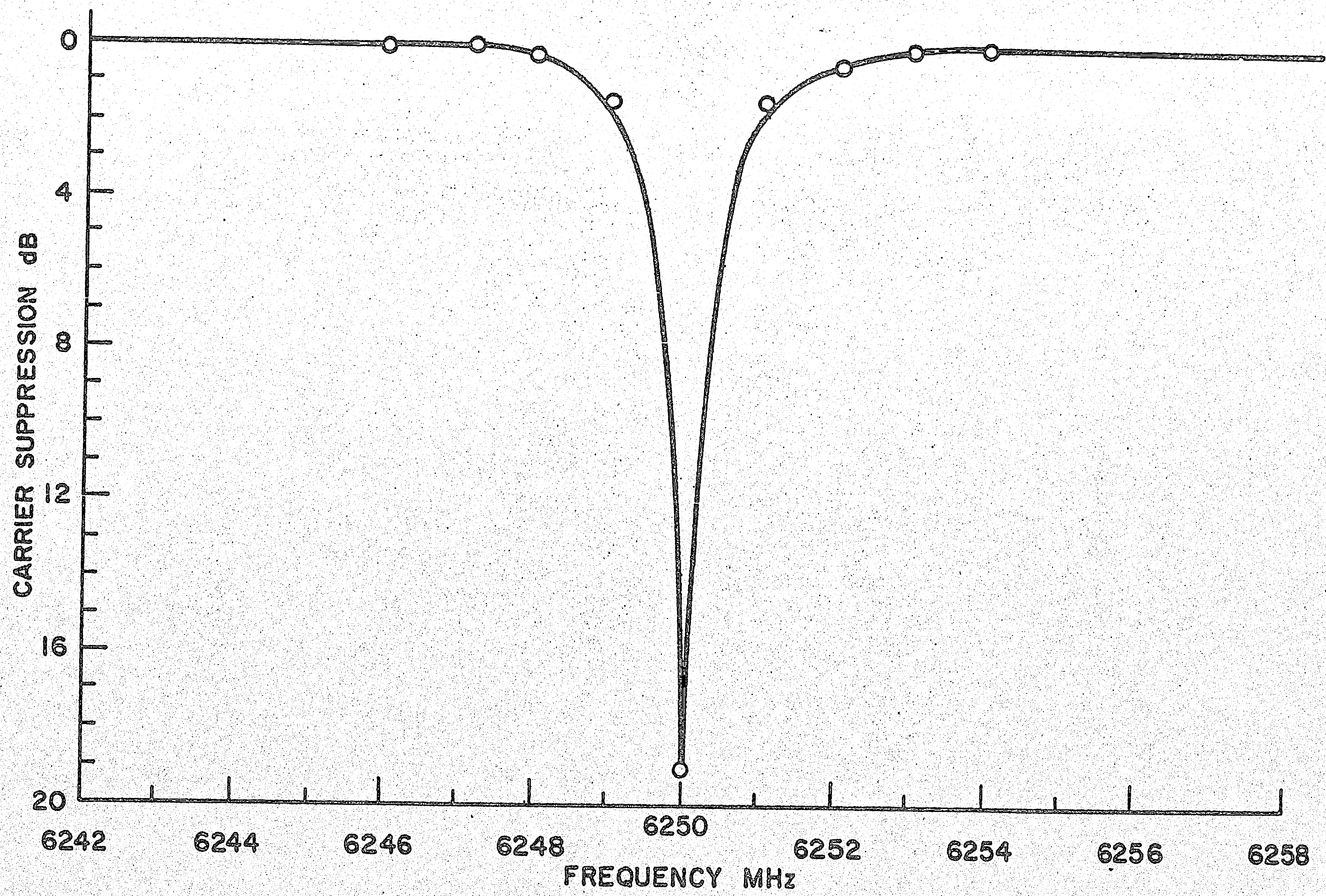


FIGURE 8 - Carrier Suppression Filter Response. The carrier suppression filter will also suppress noise close to the carrier. Corrections of 1.4 dB and 0.5 dB are necessary at one and two MHz from the carrier frequency, respectively.

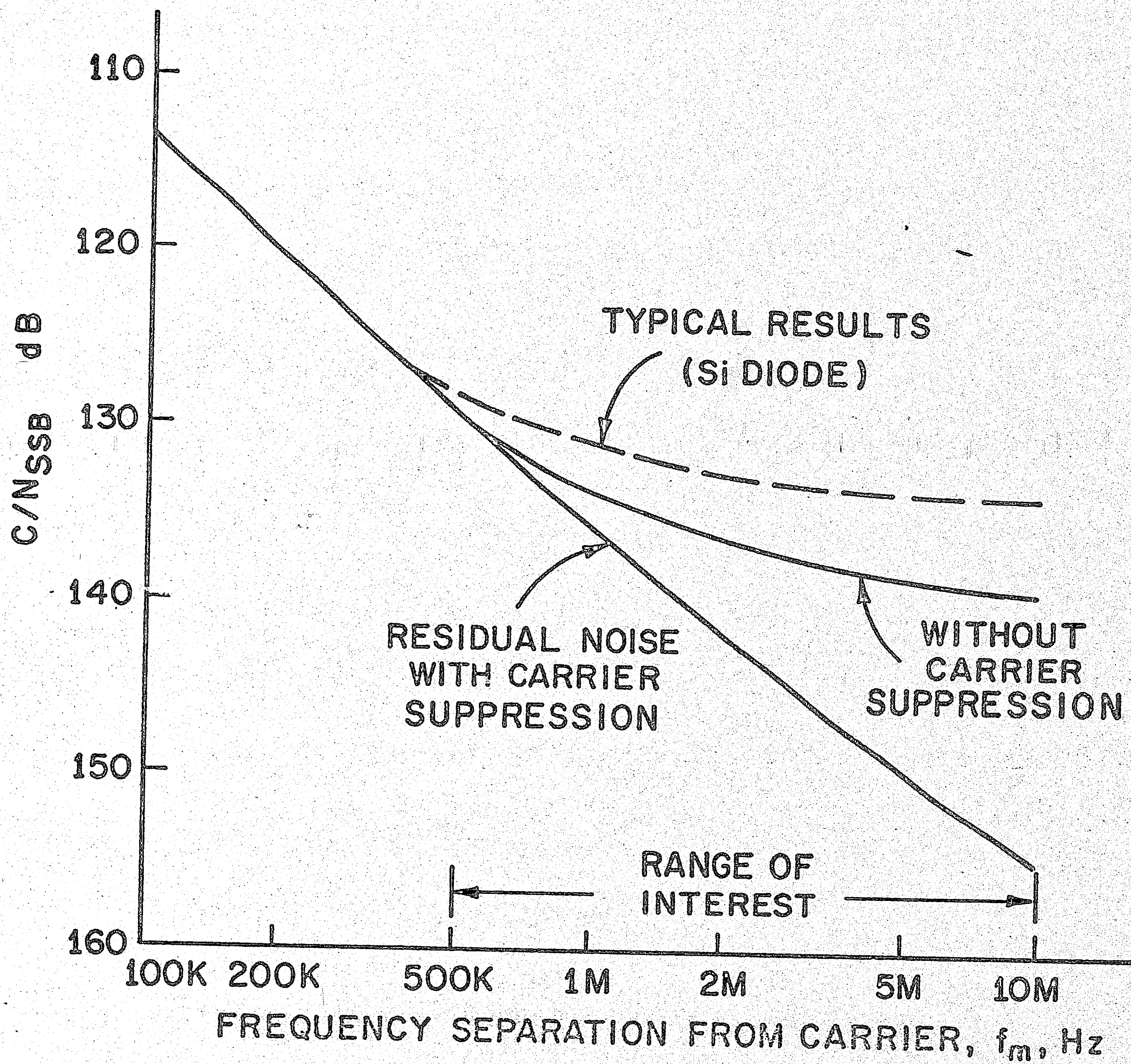


FIGURE 9 - Typical Measured Results. The dashed line shows noise as a function of baseband frequency measured using carrier suppression for a silicon IMPATT diode. The solid curves are the levels of the circuit residual noise with and without the use of carrier suppression.

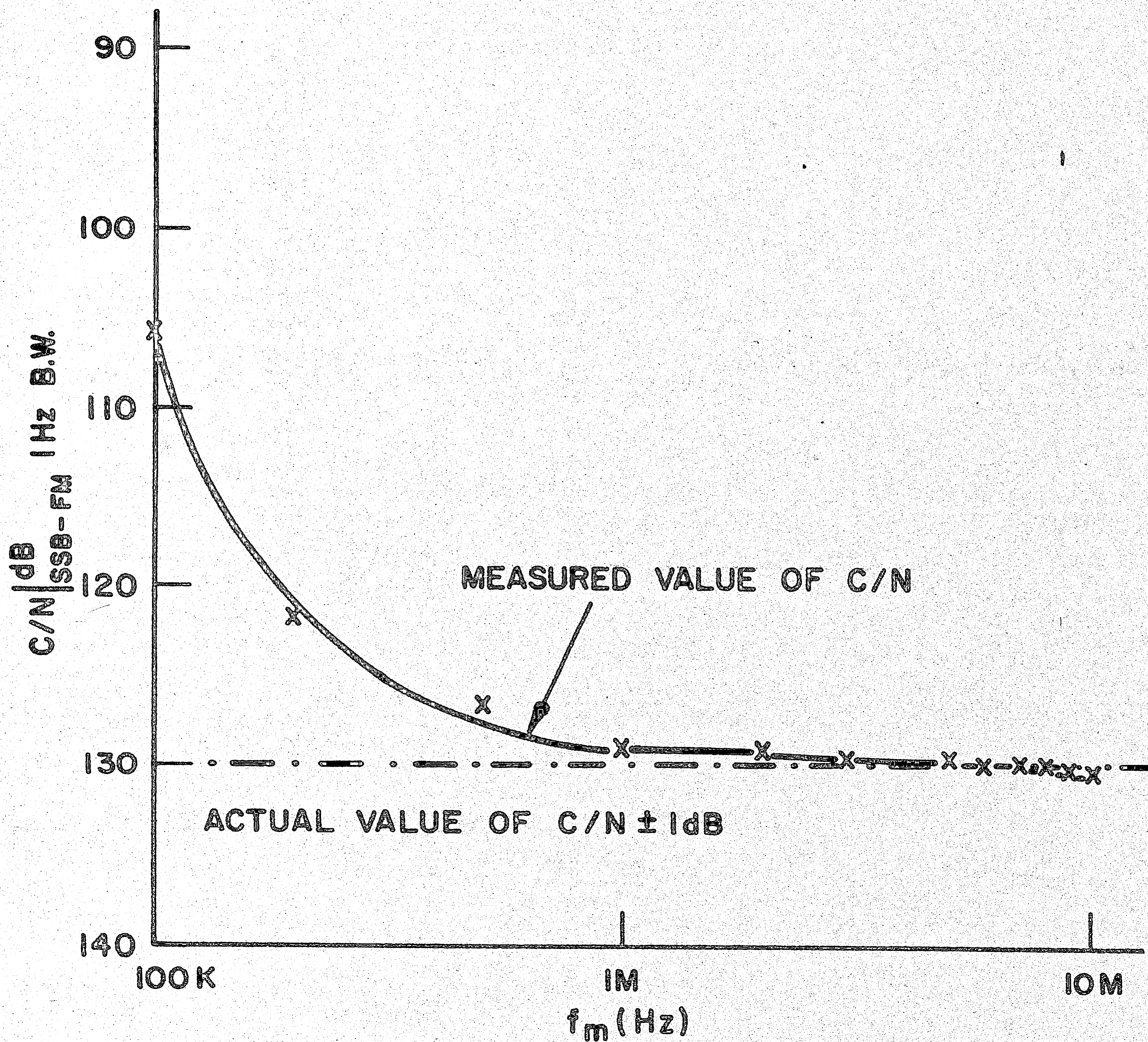


FIGURE 10 - Results of the Accuracy Test. The measured value and actual value of a known noise level are compared. The test signal level was known to within one dB. The effects of residual noise and circuit baseband "roll-off" are evident at the low and high frequency ends of the band, respectively.

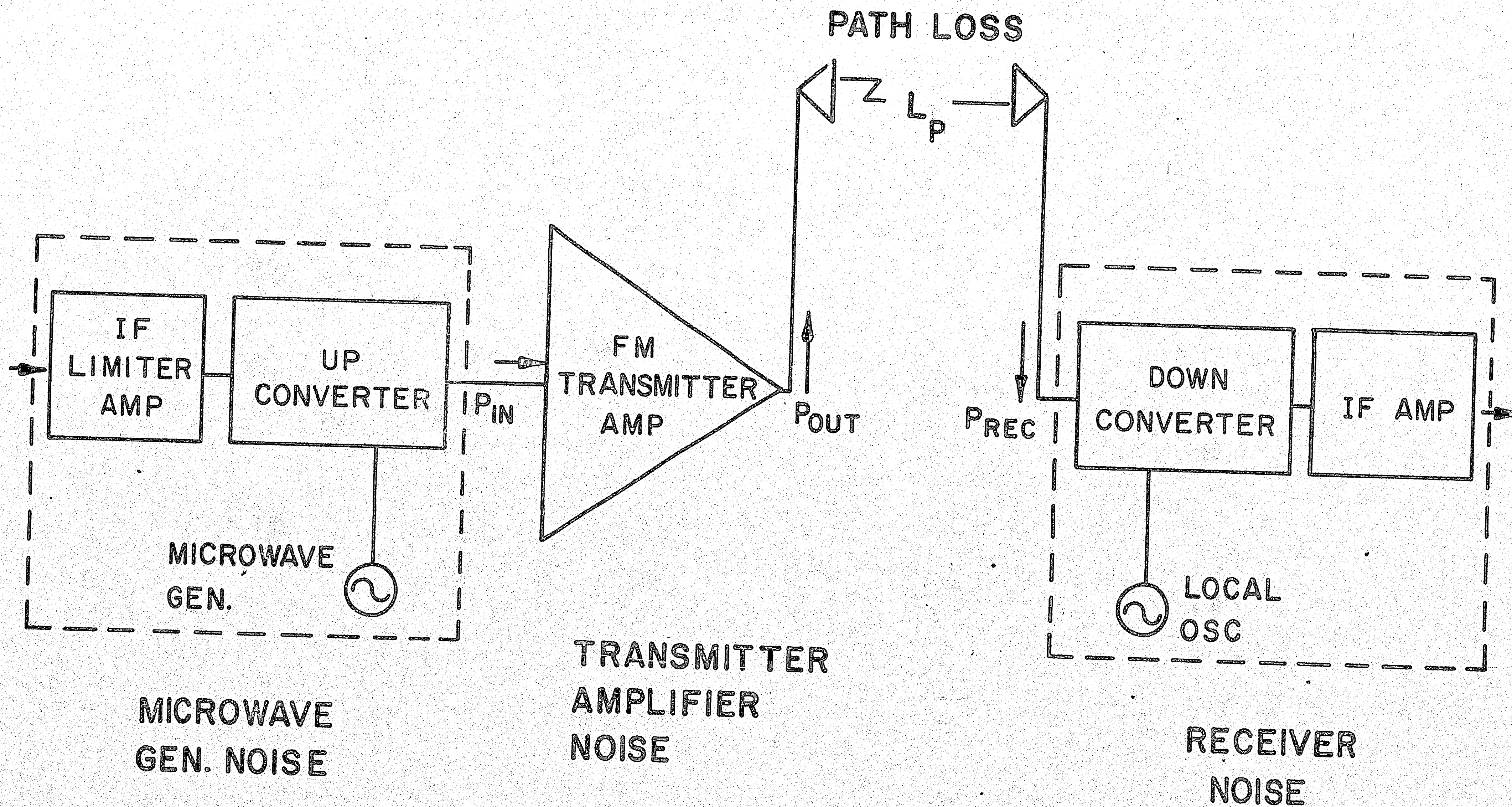


FIGURE 11 - The Assumed System Model. A single-hop of a radio relay system is shown. The assumed application is the replacement of the transmitter amplifier in an existing system design.

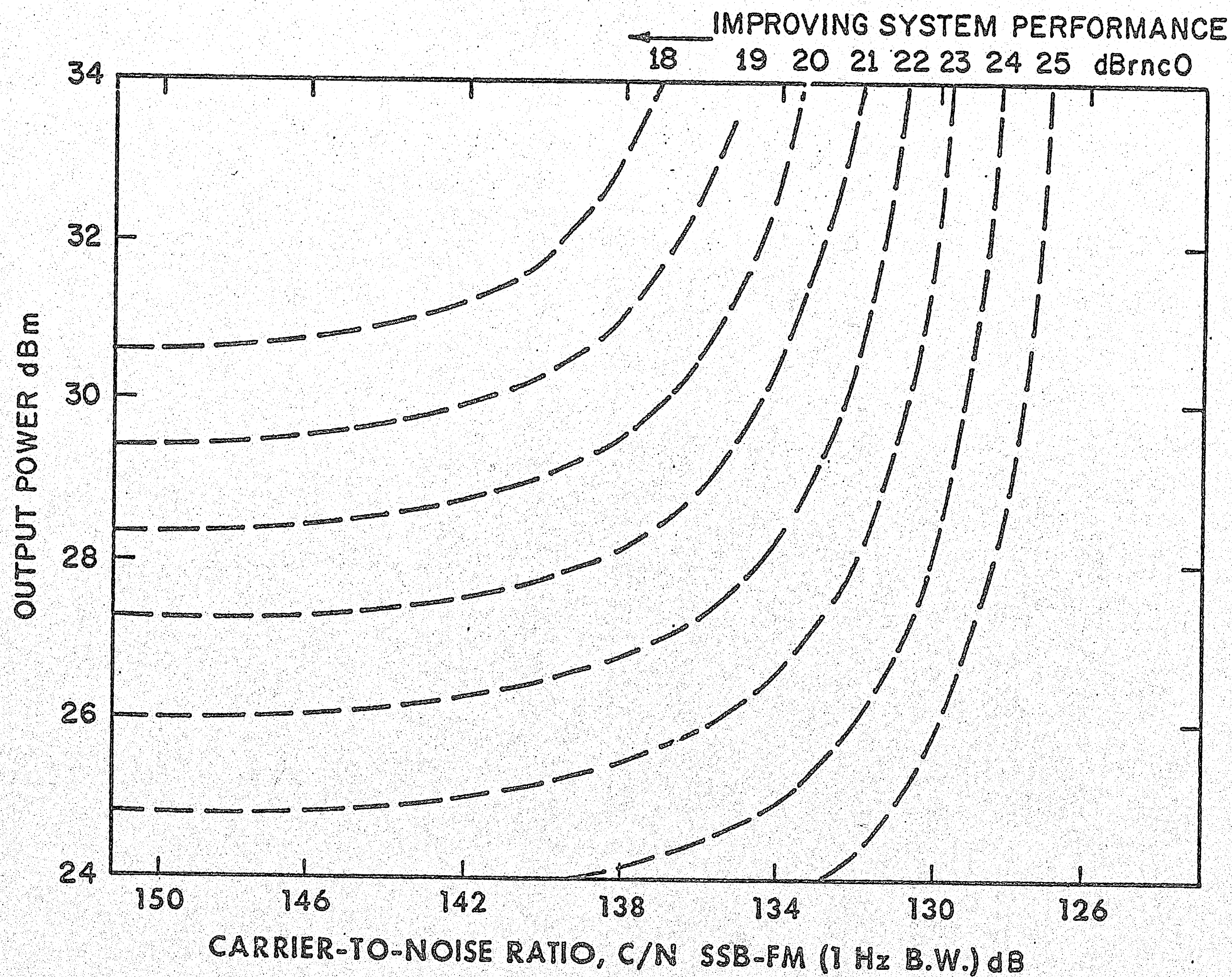


FIGURE 12 - Constant Performance Contours. Contours of constant message channel noise are plotted in the RF power-noise plane. The contours are calculated using the equations given in section 4. Typical values for the parameters were taken from an existing radio system. The message circuit noise unit is the dBrc0, the standard unit in the Bell System.

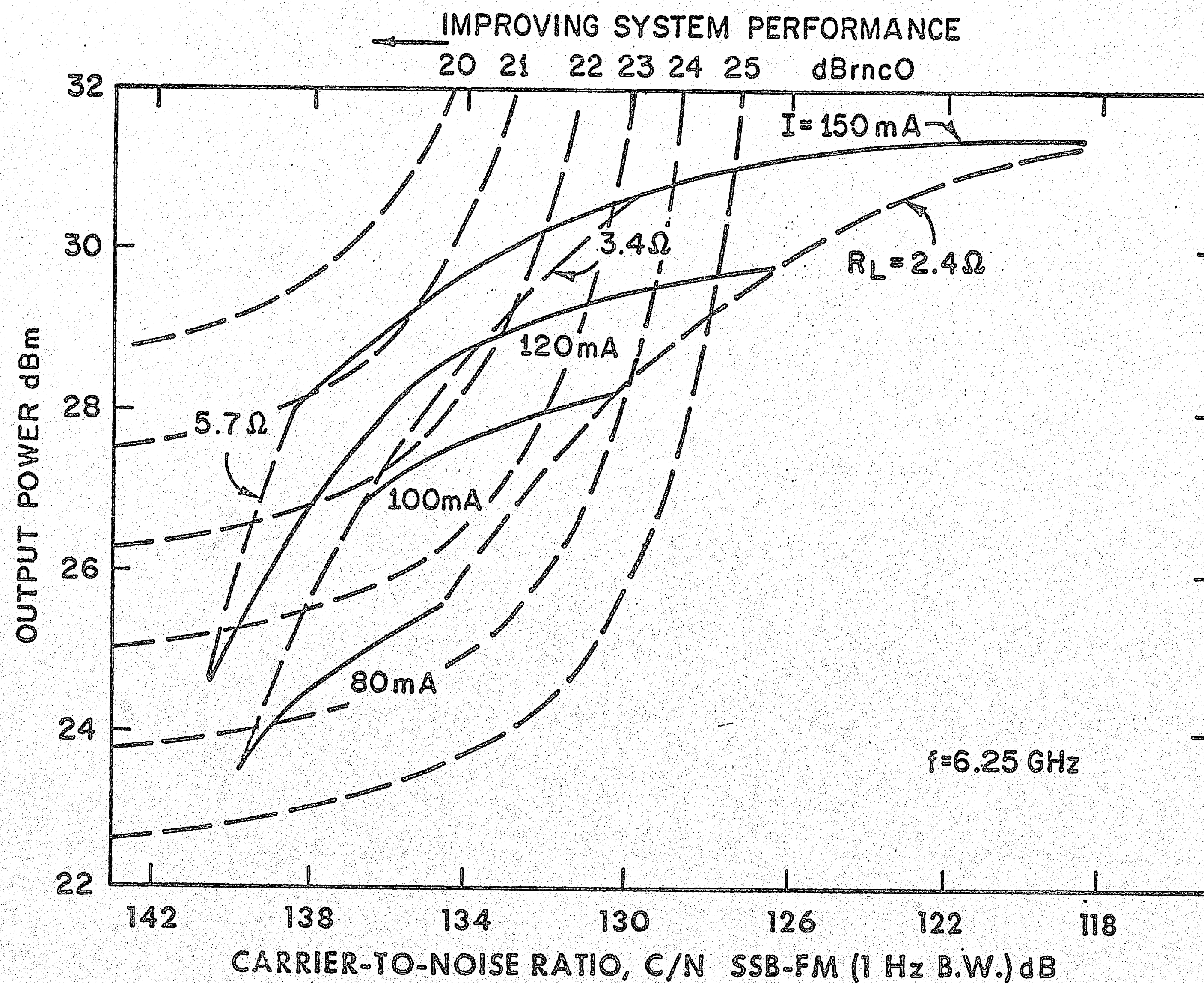


FIGURE 13 - The Prediction of System Performance. By superimposing Figures 4 and 12, this graph can be used to predict the optimum system performance (about 20.9 dB_{Brnc0} in this case). The conditions (I, R_L) which give the optimum performance with the measured diode and characterized system are also identified. The noise performance of the diode was degraded by 3 dB from Figure 4 to account for the correlation of noise sidebands.

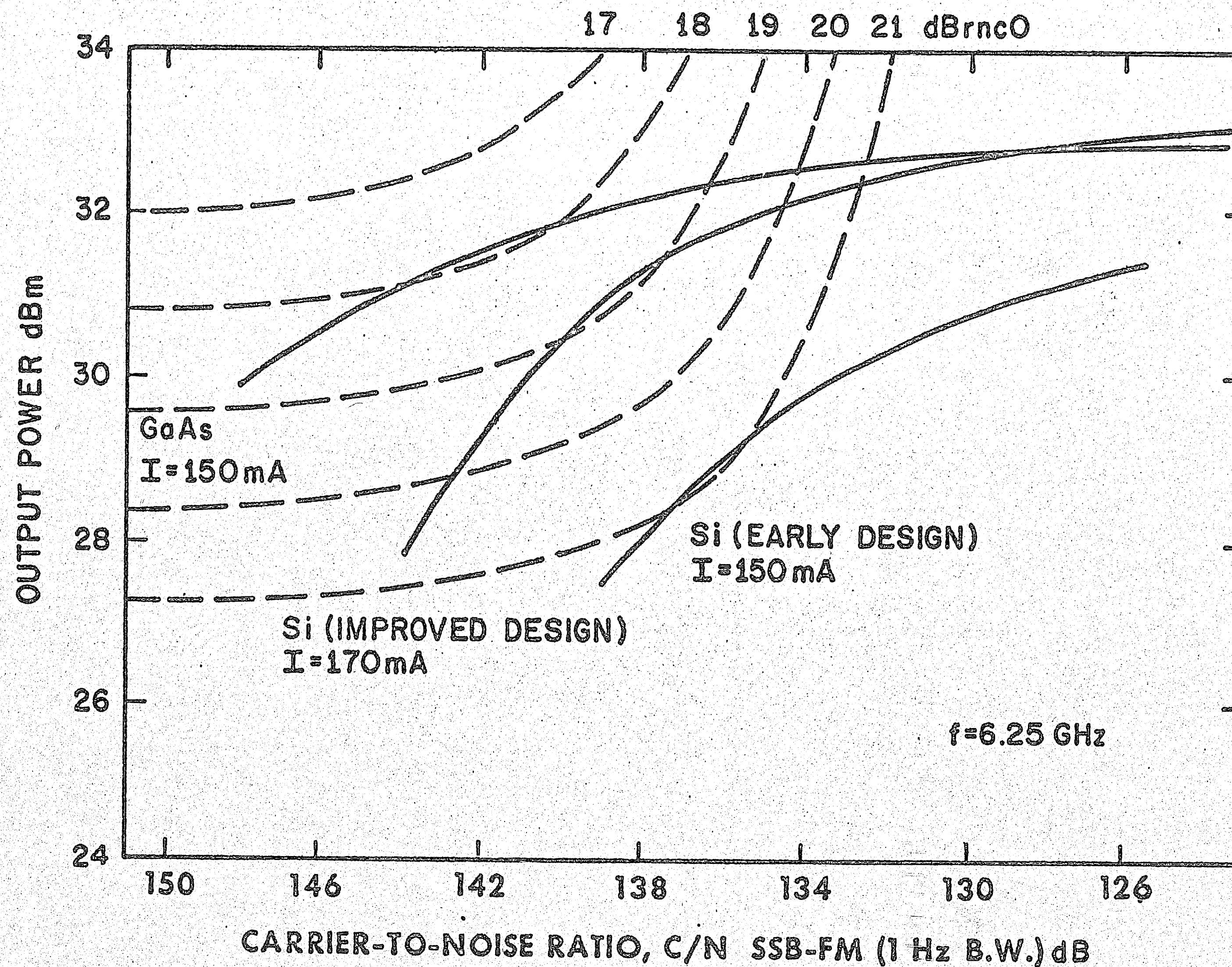


FIGURE 14 - A Comparison of Several Diodes. Comparison of the suitabilities of various diode materials or designs is possible using this technique. It is clear that an improvement in output power rather than noise is necessary for better system performance with the GaAs diode.